Integrative isotopic and molecular approach for the diagnosis and implementation of an efficient *in-situ* enhanced biological reductive dechlorination of chlorinated ethenes

Natàlia Blázquez-Pallí[a,b], Mònica Rosell[c], Joan Varias[b], Marçal Bosch[b], Albert Soler[c], Teresa Vicent[a], Ernest Marco-Urrea[a,*]

[a] Departament d'Enginyeria Química, Biològica i Ambiental, Universitat Autònoma de Barcelona (UAB), c/ de les Sitges s/n, 08193 Cerdanyola del Vallès, Spain.

[b] Litoclean, S.L., c/ Numància 36, 08029 Barcelona, Spain.

[c] Grup MAiMA, SGR Mineralogia Aplicada, Geoquímica i Geomicrobiologia, Departament de Mineralogia, Petrologia i Geologia Aplicada, Facultat de Ciències de la Terra, Institut de Recerca de l'Aigua (IdRA), Universitat de Barcelona (UB), c/ Martí Franquès s/n, 08028 Barcelona, Spain.

[*]Corresponding author:

Departament d'Enginyeria Química, Biològica i Ambiental, Universitat Autònoma de Barcelona (UAB), c/ de les Sitges s/n, 08193 Cerdanyola del Vallès, Spain. E-mail: ernest.marco@uab.cat, Phone: +34 935812694.

Total number of pages (including cover): 31

Words (including references): 7971

Figures: 6

Tables: 1

Abstract

Based on the previously observed intrinsic bioremediation potential of a site originally contaminated with perchloroethene (PCE), field-derived lactate-amended microcosms were performed to test different lactate isomers and concentrations, and find clearer isotopic and molecular parameters proving the feasibility of an *in-situ* enhanced reductive dechlorination (ERD) from PCE-to-ethene (ETH). According to these laboratory results, which confirmed the presence of *Dehalococcoides* sp. and the *vcrA* gene, an *in-situ* ERD pilot test consisting of a single injection of lactate in a monitoring well was performed and monitored for 190 days. The parameters used to follow the performance of the ERD comprised the analysis of i) hydrochemistry, including redox potential (Eh), and the concentrations of redox sensitive species, chlorinated ethenes (CEs), lactate, and acetate; ii) stable isotope composition of carbon of CEs, and sulphur and oxygen of sulphate; and iii) 16S rRNA gene sequencing from groundwater samples. Thus, it was proved that the injection of lactate promoted sulphate-reducing conditions, with the subsequent decrease in Eh, which allowed for the full reductive dechlorination of PCE to ETH in the injection well. The biodegradation of CEs was also confirmed by the enrichment in ^{13}C and carbon isotopic mass balances. The metagenomic results evidenced the shift in the composition of the microbial population towards the predominance of fermentative bacteria. Given the success of the *in-situ* pilot test, a full-scale ERD with lactate was then implemented at the site. After one year of treatment, PCE and trichloroethene were mostly depleted, whereas vinyl chloride (VC) and ETH were the predominant metabolites. Most importantly, the shift of the carbon isotopic mass balances towards more positive values confirmed the complete reductive dechlorination, including the VC-to-ETH reaction step. The combination of techniques used here provides complementary lines of evidence for the diagnosis of the intrinsic biodegradation potential of a polluted site, but also to monitor

48 the progress, identify potential difficulties, and evaluate the success of ERD at the field
49 scale.

50

51 **Keywords:** Chlorinated ethenes; Organohalide-respiring bacteria; *Dehalococcoides*; *In-*
52 *situ* pilot test; Enhanced reductive dechlorination; Carbon isotopic mass balance.

53

1. Introduction

Chlorinated ethenes (CEs) are among the most ubiquitous anthropogenic groundwater contaminants due to their widespread use in industry and recalcitrance under oxic conditions. CEs are considered priority substances (ATSDR, 2017) and have maximum contaminant levels in groundwater set by the 2008/105/EC European Directive (European Commission, 2008). Perchloroethene (PCE) is resistant to aerobic degradation but under anoxic conditions can undergo reductive dechlorination to the less-chlorinated ethenes trichloroethene (TCE), *cis*- and *trans*-dichloroethene (*cis*-, *trans*-DCE), vinyl chloride (VC), and the harmless end-product ethene (ETH).

Organohalide-respiring bacteria (OHRB) provide a potential solution to detoxify sites impacted with CEs due to their capability to use organochlorides as electron acceptors to support their growth, which result in a stepwise reduction of CEs (Bradley, 2000; Leys et al., 2013). Several OHRB can partially dechlorinate PCE to TCE or *cis*-DCE, e.g. *Geobacter* sp., but *Dehalococcoides* sp. (*Dhc*) and *Dehalogenimonas* sp. are the only genera, to date, capable of fully dechlorinating CEs to ETH (Adrian and Löffler, 2016; Yang et al., 2017b). Reductive dehalogenases (*rdh*) are the key enzymes driving organohalide respiration and can be used as biomarkers to investigate the intrinsic bioremediation potential at polluted sites (Blázquez-Pallí et al., 2019; Dugat-Bony et al., 2012; Hermon et al., 2019; Scheutz et al., 2008). Compound-specific stable isotope analysis (CSIA) can provide a complementary line of evidence to monitor biodegradation of chlorinated compounds in groundwater (Aelion et al., 2009; Hermon et al., 2018; Hunkeler et al., 1999; Nijenhuis et al., 2007; Palau et al., 2014). This technique measures a specific stable isotope ratio (e.g. $^{13}C/^{12}C$) within molecules and is based on light and heavy isotopes degrading at slightly different rates during biochemical transformations. Such shift in the isotopic composition (δ) of the molecule can be used to confirm and quantify *in-situ* biodegradation and distinguish degradation pathways (Elsner, 2010). This

is possible because the isotopic enrichment caused by physical processes such as volatilization, sorption, or dilution, is considered to be negligible (Aelion et al., 2009; Hunkeler et al., 1999). Similarly, the isotopic composition of certain non-halogenated potential electron acceptors can be used to trace changes in the redox potential of the groundwater. For instance, a dual isotope approach can be used to measure the extent of sulphate reduction because this reaction results in an enrichment in both ^{34}S and ^{18}O in the residual sulphate (Wu et al., 2011).

When OHRB are present but the electron donor becomes a limiting factor, the groundwater contaminated with CEs can show little to no dechlorination past *cis*-DCE, resulting in the accumulation of toxic intermediates (DCE or VC stall) (Bradley, 2000; Stroo and Ward, 2010). To avoid this, groundwater can be conditioned with organic fermentable substrates (e.g. lactate), which can generate reducing equivalents that promote the sequential dechlorination to ETH. This bioremediation approach is commonly referred to as biostimulation or ERD, which stands for enhanced reductive dechlorination (Adrian and Löffler, 2016; Leeson et al., 2004). To date, many studies have focused on laboratory methodologies to assess and characterize the intrinsic bioremediation potential of CEs-polluted sites by OHRB (Buchner et al., 2015; Courbet et al., 2011; Ebert et al., 2010; Kuder et al., 2013; Lee et al., 2016; Lu et al., 2009; Matteucci et al., 2015; Nijenhuis et al., 2007; Slater et al., 2001; Tarnawski et al., 2016; Yu et al., 2018), but few have reported results after applying ERD and CSIA at the field scale (Herrero et al., 2019; Hirschorn et al., 2007; Song et al., 2002).

The research reported in Blázquez-Pallí et al. (2019) presented a multi-method approach to assess the intrinsic biodegradation potential of an industrial site in Barcelona (Spain) polluted by CEs. Obtained results discouraged natural attenuation as a remediation strategy due to *cis*-DCE stall, and recommended an ERD injecting lactate as electron donor. In line with those conclusions, the present study aimed at continuing the

remediation work at that same aquifer and apply an integrated isotopic and molecular approach that provides complementary lines of evidence to implement, monitor and assess an efficient *in-situ* biodegradation of CEs at the site during an ERD. To this end, a more detailed laboratory study focusing, as well, on the concentration and isomeric form of lactate required for the complete dechlorination of PCE to ETH was performed first, followed by the monitoring of the *in-situ* ERD pilot test and the final full-scale treatment. The used methodology in all cases combined (1) the acquisition of hydrogeochemical data, (2) microcosms experiments, (3) molecular techniques (i.e. identification of selected biomarkers and 16S rRNA high-throughput sequencing of groundwater samples), and (4) stable isotopes of sulphate (as model redox sensitive species), and carbon from the target contaminants (CEs).

2. Materials and methods

2.1. Chemicals

PCE (99.9% purity) was from Panreac; laboratory-grade sodium DL-lactate (≥98% purity) from Sigma-Aldrich (hereinafter, Lactate-1), and food-grade sodium L-lactate (97% purity, at 60% w/w) from Purac (Corbion) (hereinafter, Lactate-2). Other chemicals and reagents used for the present study were purchased from Sigma-Aldrich, Thermofisher and Bio-Rad at scientific grade or higher.

2.2. Study site

The studied site is located in the Barcelona province (Spain) and the aquifer is mainly constituted by three lithological units: i) a lower layer of reddish clay loams, ii) an intermediate layer of brown and silty clays, and iii) an upper layer of ochre silty clays. Given such lithology, the hydraulic conductivity is generally low, only improved by localized gravel and sandstone areas that increase the permeability of the media and could act as preferential flow paths. A hydrogeological cross section of the site is depicted in

Figure S1, and a more detailed description of the aquifer can be found elsewhere (Blázquez-Pallí et al., 2019). A preliminary site characterization revealed a significant PCE plume, accompanied by minor amounts of TCE, *cis*-DCE and VC. Originally, it was treated by a combination of pump and treat (P&T) and dual-phase extraction (DPE, vapour and groundwater). Pumped groundwater was later treated through an air stripping system. Groundwater flowed naturally in the NW–SE direction (Figure 1); however, under such ongoing remediation, all the extraction points were almost dried due to the low productivity of the aquifer. These P&T and DPE systems were halted partially during the *in-situ* pilot test (only remained active in some wells outside the pilot test area), and completely for the full-scale bioremediation. However, certain influence of this pumping on the groundwater flow direction during the *in-situ* pilot test cannot be discarded.

2.3. Microcosm experiments

Groundwater with fine sediments was collected from the intended pilot scale injection well PZ-2 (Figure 1) with a peristaltic pump on October 4th, 2016, in transparent sterile glass bottles that were sealed with PTFE caps as described elsewhere (Blázquez-Pallí et al., 2019). These groundwater samples were kept in the dark at 4ºC until the following day, when microcosms were set up. Four different treatments were prepared, at least in duplicate: (1) control containing only groundwater, (2) groundwater with Lactate-1 at ~ 3 mM, (3) groundwater with Lactate-2 at ~ 3 mM, and (4) groundwater with Lactate-2 at ~ 15 mM. Each 100 mL microcosm bottle contained 65 mL of sampled groundwater with fine sediments and the lactate concentrations described above. All microcosms were prepared in an anoxic glovebox and incubated in the dark at 25 °C. Microcosms that fully dechlorinated CEs were reamended with TCE and transferred to sterilized anoxic synthetic medium (3–7% v/v) described elsewhere (Martín-González et al., 2015) during the exponential degradation phase of CEs.

For the analysis of the site-specific carbon isotopic fractionation (εC) during degradation of PCE, six parallel anoxic cultures were prepared with the abovementioned defined medium and groundwater from PZ-2 (1.5% v/v) as inoculum. Each culture was spiked with PCE (235 µM), and sacrificed with NaOH (10 M) at 0, 1, 6, 77, 88, 96 and 97% of PCE degradation. Three different controls were prepared in duplicate: (1) killed controls with PCE, (2) killed controls without PCE, and (3) abiotic controls with PCE.

2.4. Implementation of the ERD in-situ pilot test

The pilot test consisted of a unique injection of lactate at well PZ-2 (Figure 1) on October 25th, 2016 (t_0). The product injected was an aqueous solution of Lactate-2 diluted with groundwater outflowing from the air stripping system installed at the site. The total volume of substrate injected was lower than 10% of the treatment zone volume. The design parameters of the *in-situ* pilot test were based on the recommendations from Leeson et al. (2004) and Dugat-Bony et al. (2012).

2.5. Monitoring of the ERD in-situ pilot test

Field parameters (i.e. Eh, pH, T, and electric conductivity (EC)) were measured *in-situ* and groundwater was collected with a peristaltic pump from the injection well PZ-2 and nearby wells PZ-1, PZ-3, PZ-6, PZ-22, MW-6, and Prof.D (Figure 1) as described elsewhere (Blázquez-Pallí et al., 2019). Sampling campaigns were carried out the day before injection of lactate (t_{-1}, October 24th, 2016) and the next 2, 9, 20, 50, 86, 142 and 190 days after the injection (hereinafter, t_i). Samples collected for both CSIA and CEs concentration were immediately killed with NaOH (pH>10) and stored at 4ºC until analysed. Short-chain volatile fatty acids (VFAs) were analysed from groundwater samples filtered on site (0.20 µm) and stored in borosilicate tubes at 4ºC until analysed.

2.6. Isotopic evaluation of the full-scale ERD treatment

A full-scale ERD treatment was implemented by Litoclean, S.L. on August 2017. The bioremediation strategy consisted in the injection of Lactate-2 every three months for the

period of a year. Between 30 and 50 out of a total of 66 monitoring wells at the site were used for the injection of the substrate at every event but changing the distribution of the injections to ensure the maximum coverage of the plume area. On September 2018, after one year of treatment, groundwater was sampled from wells PZ-3, PZ-5, PZ-22, MW-3, MW-6, and MW-7 (Figure 1) following the same methodology mentioned in section 2.5. Samples were analysed for CEs concentrations and CSIA, and data were compared to previous (before the *in-situ* pilot test) chemical and isotopic values for each well.

2.7. Analytical methods

CEs concentrations were analysed from 500 µL headspace samples by gas chromatography (GC) coupled to a flame ionization detector (FID) as reported by Martín-González et al. (2015). VFAs (lactate, pyruvate, acetate, formate) were analysed by high performance liquid chromatography (HPLC) from filtered liquid samples as described elsewhere (Mortan et al., 2017).

Stable carbon isotopes of CEs were analysed with an Agilent 6890 GC coupled to an IRMS at *Centres Científics i Tecnològics de la Universitat de Barcelona* (CCiT-UB), following the procedure described in Blázquez-Pallí et al. (2019). Carbon isotopic compositions in all samples are presented in delta notation (δ^{13}C, in ‰), relative to the international standard Vienna Pee Dee Belemnite (VPDB), following

$$\delta^{13}C = \left(\frac{R_{sample}}{R_{std}} - 1\right) \cdot 1000 \qquad (1)$$

where R_{sample} and R_{std} represent the isotope ratios (e.g. $^{13}C/^{12}C$) of the sample and the standard, respectively (Elsner, 2010). Instrument uncertainty was considered as the standard deviation (1σ) of duplicate measurements. For field data, the degradation is considered significant if the shift in δ^{13}C is >2‰ compared to its original value (Hunkeler et al., 2008).

Carbon isotopic mass balance for CEs at each monitoring well was calculated according to Aeppli et al. (2010) and Hunkeler et al. (1999), as follows

$$\delta^{13}C_{sum} = x_{PCE} \cdot \delta^{13}C_{PCE} + x_{TCE} \cdot \delta^{13}C_{TCE} + x_{DCE} \cdot \delta^{13}C_{DCE} + x_{VC} \cdot \delta^{13}C_{VC} \quad (2)$$

where *x* is the molar fraction of each substance with respect to the total molar mass (sum of CEs for which δ^{13}C values were available) for each sample at each sampling event. In this case, as PCE was the only contaminant spilled in this aquifer, the $\delta^{13}C_{sum}$ must remain constant as long as (1) PCE released along the time and space had the same isotopic composition, (2) the unique transformation pathway was reductive dechlorination, (3) VC does not further degrade to ETH when considered in the balance (Aeppli et al., 2010; Hunkeler et al., 1999; Palau et al., 2014).

The logarithmic form of the simplified Rayleigh equation correlates changes in the carbon isotope ratios (R_t/R_0) and changes in concentrations ($f=C_t/C_0$) with time for a closed system (Elsner, 2010), and the obtained epsilon (εC) represents the carbon isotopic fractionation, as follows

$$\ln\left(\frac{R_t}{R_0}\right) = \varepsilon C \cdot \ln(f) \quad (3)$$

where R_t/R_0 can be expressed as $(\delta^{13}C_t + 1) / (\delta^{13}C_0 + 1)$.

The analysis of major anions (HCO_3^-, NO_3^-, Cl^-, SO_4^{-2}) and cations (Na^+, K^+, Ca^{+2}, Mg^{+2}) was performed at CCiT-UB. Total concentrations of Na^+, K^+, Ca^{+2}, Mg^{+2} were analysed by inductively coupled plasma-optic emission spectrometry (ICP-OES, Optima 3200 RL) and by inductively coupled plasma mass spectrometry (ICP-MS, Elan 6000). NO_3^-, Cl^-, and SO_4^{-2} concentrations were determined by HPLC using a WATERS 515 HPLC pump with an IC-PAC anion column and a WATERS detector (mod 432), while HCO_3^- was measured by titration (METROHM 702SM Titrino). The predominant

equilibrium systems controlling the Eh were investigated via Eh–pH predominance diagrams prepared with the MEDUSA code (Puigdomènech, 2010).

Dissolved SO_4^{-2} detected in groundwater was precipitated as $BaSO_4$ as reported elsewhere (Dogramaci et al., 2001) and its sulphur and oxygen isotopic compositions were analysed following Rodríguez-Fernández et al. (2018). Results are presented in delta notation (δ^{34}S-SO_4^{-2} and δ^{18}O-SO_4^{-2}, in ‰), relative to the international standards, Vienna Standard Mean Oceanic Water (VSMOW) for δ^{18}O and Vienna Canyon Diablo Troillite (VCDT) for δ^{34}S.

2.8. DNA extraction, PCR and 16S rRNA gene high-throughput sequencing

DNA for molecular analyses was extracted from TCE-enriched field-derived cultures (three transfers into fresh synthetic medium) that were originally amended with Lactate-2 (~ 3 mM) and from well PZ-2. Cell harvesting, genomic DNA isolation and PCR reaction for amplification of the *vcrA* gene were performed as described in Blázquez-Pallí et al. (2019). Primer sets used are detailed in Table S1.

To investigate the OHRB involved in the biodegradation of CEs to ETH, the dilution-to-extinction method (Löffler et al., 2005) was applied in 20-mL vials containing 12 mL of the anoxic synthetic medium mentioned in section 2.3, but using 1 mL of active TCE-enriched field-derived culture as inoculum and *cis*-DCE as electron acceptor. After three extinction series, the more diluted vial showing ETH formation was used as inoculum for serum bottle microcosms and, after consuming 10 µM *cis*-DCE, was selected for 16S rRNA analysis. After DNA extraction, amplicons of the region V3–V4 for 16S rRNA genes were amplified with primers S-D-Bact-0341-b-S-17 and S-D-Bact-0785-a-A-21 (Klindworth et al., 2013) with the Illumina MiSeq sequencing platform at *Serveis de Genòmica i Bioinformàtica* from *Universitat Autònoma de Barcelona* (Spain).

To characterize the impact of the injection of lactate on the bacterial community

structure after the *in-situ* pilot test, 80 mL of groundwater were collected from wells PZ-2, PZ-1, and PZ-22 at t_{-1} and t_{142}. Samples were stored at -20ºC until DNA extraction and 16S rRNA gene high-throughput sequencing were performed at AllGenetics & Biology (A Coruña, Spain). For DNA extraction, samples were centrifuged at 5000 *g* for 1 h and the pellet was transferred to PowerBead tubes of the DNeasy Powersoil DNA isolation kit (Qiagen). DNA was isolated following the instructions of the manufacturer. For library preparation, a fragment of the bacterial 16S rRNA region of around 450 bp was amplified using primers Bakt_341F and Bakt_805R (Herlemann et al., 2011). The pool was sequenced in a MiSeq PE300 run (Illumina).

3. Results and discussion

3.1. Feasibility and markers for complete ERD at laboratory scale

3.1.1. Assessment of the lactate isomers and concentration in microcosm experiments

Microcosms were prepared to test whether reductive dechlorination of CEs to ETH was feasible in the injection well PZ-2. Besides the control, which accounted for monitored natural attenuation (MNA), two different isomeric forms of sodium lactate (DL-/Lactate-1 and L-/Lactate-2) were used to test their effect on the lactate fermentation potential of the native microbial community. Moreover, Lactate-2 was used because it was a candidate product in a foreseeable *in-situ* pilot test. Accordingly, Lactate-2 was amended at two different concentrations to discard inhibition effects. On the one hand, the unamended controls transformed PCE to *cis*-DCE and VC within 15 days, but ETH was not detected. When microcosms were reamended with TCE (35 µM) at day 25, dechlorination barely passed VC, and ETH was detected at low concentration after 50 days (Figure S2A). On the other hand, lactate-amended treatments fully dechlorinated PCE to ETH within 15 days and exhibited similar rates independently of the isomeric form and concentration (Figure S2, B–D). After adding TCE in all three of them at days

25 and 45, the dechlorination remained active with the consequent accumulation of ETH (Figure S2, B–D). In all amended microcosms, lactate was totally consumed and acetate was produced within 10 days (data not shown). However, excess of electron donor and, thus, of H_2, did promote methanogenesis, resulting in a vigorous formation of methane in the microcosm with ~ 15 mM of lactate (Figure S3), which has been reported before (Blázquez-Pallí et al., 2019; Leeson et al., 2004).

3.1.2. Identification of *vcrA* gene and CEs dechlorinating bacteria

PCR amplifications with the *vcrA* gene-targeted primer were run to investigate whether the *vcrA* gene was present in the TCE-enriched field-derived cultures from well PZ-2 (section 2.8). After gel electrophoresis, observed diagnostic amplicons indicated that the culture contained *vcrA* gene, which is implicated in the VC-to-ETH dechlorination step (Figure S4).

In these TCE-enriched cultures, three dilution-to-extinction series were applied using *cis*-DCE as electron acceptor to get insight into the OHRB responsible for ETH generation. The 16S rRNA gene amplicon sequencing and the taxonomic assignments revealed that the four predominant genera were *Pleomorphomonas* (50%), described as nitrogen-fixing bacteria (Im et al., 2006; Madhaiyan et al., 2013; Xie and Yokota, 2005); *Desulfomicrobium* (18%), which are sulphate-reducing bacteria (Sharak Genthner et al., 1997, 1994); and the OHRB *Geobacter* (14%) and *Dehalococcoides* (3%) (Figure 2). *Geobacter* sp. can derive energy from acetate oxidation coupled to PCE-to-*cis*-DCE dechlorination, but it is also capable of growing on a wide range of non-halogenated electron acceptors (Atashgahi et al., 2016; Sanford et al., 2016). The presence of *Dehalococcoides* was consistent with the detection of *vcrA* reductive dehalogenase gene (Figure S4) and ETH generation in lactate-amended microcosms (Figure S2).

306 3.1.3. Site-specific εC for PCE degradation

307 The analysis of site-specific εC can help estimate the extent of the *in-situ*
308 biodegradation of contaminants in the field (Elsner, 2010). PCE was depleted in the
309 microcosms inoculated with groundwater from PZ-2 (Figure S5A) but dechlorination was
310 not accompanied by a significant change in its isotopic composition ($\delta^{13}C_{PCE}$) (Figure
311 S5B). In more detail, $\delta^{13}C_{PCE}$ shifted only 0.81‰ and 1σ for duplicate measurements
312 were, for all samples, below total instrumental uncertainty of 0.5‰ (Sherwood Lollar et
313 al., 2007). The dechlorination reaction did not fit the Rayleigh model (Eq. 3, $R^2 = 0.63$,
314 $\varepsilon C = -0.2 \pm 0.2‰$), which deemed this site-specific εC as not significant (ns). In contrast,
315 a stronger enrichment in ^{13}C was observed when the produced TCE was further degraded
316 to *cis*-DCE (Figure S5B). This non-linear εC for PCE is, most likely, the combined effect
317 of several OHRB simultaneously transforming PCE, with a major contribution of the non-
318 fractionating species. This agrees with the predominance of *Geobacter* sp. in the cultures
319 (Figure 2), which is reported to have a non-significant εC for PCE and could have lead
320 the PCE-to-TCE dechlorination (Table S2) (Cichocka et al., 2008). Abiotic and NaOH-
321 killed controls did not show PCE losses or degradation as its concentration did not vary
322 significantly throughout the whole experiment (236 ± 8 μM, n=6, Figure S5A) and no
323 degradation products were detected.

324 *3.2. In-situ ERD pilot test with lactate at the injection well PZ-2*

325 Microcosms of PZ-2, which mimicked the natural attenuation conditions at the site,
326 indicated that reductive dechlorination could stall at an intermediate stage, resulting in an
327 accumulation of *cis*-DCE and VC (Figure S2A). However, the amendment of lactate
328 resulted in a faster dechlorination of PCE and concomitant generation of ETH (Figure S2,
329 B–D). Considering these results, an *in-situ* ERD pilot test with Lactate-2 was
330 implemented at well PZ-2.

331 3.2.1. Hydrochemistry changes induced by the lactate injection

332 The concentration of major anions (SO_4^{-2}, NO_3^-, HCO_3^-, Cl^-) and cations (Na^+, K^+,
333 Ca^{+2}, Mg^{+2}) was analysed at t_{-1}, t_{20}, t_{86} and t_{190}. At the injection well PZ-2, NO_3^- and SO_4^{-2} were depleted after the addition of the Lactate-2 solution (Figure S6A), whereas Na^+,
335 Ca^{+2}, Mg^{+2} and electric conductivity (EC) increased, responding to the injected electron
336 donor (Table S3). At the monitoring wells PZ-1, PZ-6 and MW-6, NO_3^- concentrations
337 were depleted as well, but different trends were observed for SO_4^{-2} (Figure S6, A and B).
338 In contrast, no significant changes were observed for those anions in monitoring wells
339 PZ-3, PZ-22, and Prof.D (Figure S6C).

340 Geochemical modelling shows that the aquifer was at nitrate-reducing conditions
341 before injection and that the addition of lactate promoted a shift towards sulphate-
342 reducing and methanogenic conditions (Figure S7). This shift was more extreme in the
343 injection well PZ-2 (at t_{20}) as well as in monitoring wells PZ-1 (at t_{86}), and PZ-6 and MW-
344 6 (both at t_{190}), which agrees with the decrease observed in NO_3^- and SO_4^{-2} concentrations
345 (Figure S6). In addition, results suggested that the system was controlled by calcite
346 ($CaCO_3$(s)) (Figure S7B), as the pH was maintained within the range of 6–8, the optimal
347 for OHRB (Yang et al., 2017a).

348 $\delta^{34}S$ and $\delta^{18}O$ values of dissolved SO_4^{-2} from t_{-1} at each monitoring well were
349 compared with the ones obtained after the lactate injection (t_{20}, t_{86} or t_{190}). Before the
350 injection, the S and O isotopic composition of SO_4^{-2} at the site showed diverse values
351 corresponding to a mixture among geogenic composition (Triassic or Tertiary recycled
352 gypsum) in well Prof.D, synthetic fertilizers, and an unknown source (with the lowest ^{34}S
353 and ^{18}O values) that could be related to agricultural uses of manure (Otero et al., 2008).
354 This variability points out to a heterogeneity in the origin of the dissolved sulphate in the
355 aquifer (Figure 3). In any case, in the injection well PZ-2, isotopic compositions at t_{20}
356 became significantly more enriched with a shift of $\Delta\delta^{34}S$ = +3.0‰ and $\Delta\delta^{18}O$ = +3.2‰

resulting in a slope of 1.1 (Figure 3). These $\delta^{34}S$ and $\delta^{18}O$ values of sulphate seem influenced by the mixing with the sulphate isotopic composition of the injected water (Figure 3). Unluckily, no values could be obtained for t_{86} or t_{190} due to concentrations being below the limit of quantification. An even larger shift was measured in monitoring wells PZ-6 and MW-6 because the slower decrease of SO_4^{-2} concentrations allowed the measurement of more points. By t_{190}, PZ-6 showed the most ^{34}S enriched value measured at the site, also with respect to its t_{-1} ($\Delta\delta^{34}S$ = +14.4‰), but with a small $\delta^{18}O$ enrichment ($\Delta\delta^{18}O$ = +1.0‰) (Figure 3). For MW-6, the most enriched $\delta^{34}S$ was measured in t_{86} ($\Delta\delta^{34}S$ = +7.4‰), while the largest $\Delta\delta^{18}O$, of +4.7‰, was measured in t_{190} (Figure 3). In contrast, $\Delta\delta^{34}S$ and $\Delta\delta^{18}O$ in monitoring wells PZ-1, PZ-3, PZ-22, and Prof.D were not significant (Figure 3). A wide variation in the dual S–O slopes have been described for bacterial sulphate reduction in different natural environments (from 0.23 to 1.7) (Antler et al., 2013; Mizutani and Rafter, 1973). These differences have been linked to the net sulphate reduction rate and to the recycling of intermediate species (such as sulphite that facilitate oxygen isotope exchange with H_2O) back to sulphate. In environments where sulphate reduction is fast, this sulphite re-oxidation is minimal resulting in lower slopes due to sulphur isotopes increasing faster than oxygen isotopes (Antler et al., 2013). Thus, obtained results (with the available data points) proved sulphate reduction after lactate injection only in PZ-6 and MW-6 by isotopic enrichment rather than pure mixing with injected water.

3.2.2. Enhanced biodegradation of chlorinated ethenes at the injection well PZ-2

PCE was the main toxic substance dissolved in groundwater of PZ-2 before lactate injection (Figure 4A). After biostimulation, Eh decreased from +300-400 mV to ~ -50 mV by t_{20} (Figure 4D) and acetate was detected for the first time by t_{50} (Figure 4C). The generation of reducing equivalents from lactate fermentation and the subsequent dramatic decrease of Eh favoured dechlorination past *cis*-DCE and VC up to ETH by t_{190} (Figure

383 4A). The full dechlorination of CEs to ETH by t_{190} was also confirmed by the enrichment
384 in the isotopic mass balance ($\delta^{13}C_{sum}$), which changed from -33 ± 2‰ to -9.0 ± 0.5‰
385 (Figure 4B). This difference in the $\delta^{13}C_{sum}$ is due to not considering the isotopic
386 composition of ETH after VC degradation (which would be depleted as lighter isotopes
387 react faster). Hence, $\delta^{13}C_{sum}$ became less negative as VC to ETH reaction progressed. In
388 detail, the PCE to TCE reaction at PZ-2 did not change $\delta^{13}C_{PCE}$ significantly and remained
389 constant throughout the whole monitoring period (Figure 4B), emulating the results of
390 the microcosm experiments (εC = ns) (section 3.1.3.). Conversely, TCE and *cis*-DCE
391 showed variations in $\delta^{13}C$ during the *in-situ* dechlorination process, which were up to
392 +7‰ for TCE and +16‰ for *cis*-DCE at the measured times (Figure 4B). Lastly, VC
393 could be nicely traced, exhibiting a remarkable variation of $\delta^{13}C$ (shift up to +49‰)
394 including its formation from *cis*-DCE and degradation to ETH by t_{190} (Figure 4B).

395 3.2.3. Impact of the *in-situ* ERD pilot test at wells within the direct radius of influence

396 Lactate and/or acetate were progressively detected in PZ-1 (at t_2), PZ-6 (at t_{20}) and
397 finally in MW-6 (at t_{142}), indicating the arrival of the injected solution through the
398 preferential groundwater flow paths (with a stronger N–S direction than at natural
399 conditions, Figure 1), thus drawing the direct radius of influence of the *in-situ* ERD pilot
400 test. Another evidence of the affectation at these wells was the dramatic decrease in Eh
401 like the one observed in the injection well PZ-2 (Figures S8, S9, S10). However, even
402 when reaching similar negative Eh values (down to -100 mV), the PCE reductive
403 dechlorination mainly stalled at *cis*-DCE (most evident in PZ-1) (Figures 5, S8, S9, S10),
404 while in PZ-6 (farther from PZ-2) *cis*-DCE started to pass to VC and ETH by t_{190} (Figure
405 S9A). These concentration data agree with $\delta^{13}C_{sum}$ of CEs remaining constant in the three
406 wells (~ -32‰ over 190 days, Figures 5, S8B, S9B, S10B), so there was no significant
407 alternative degradation pathways besides ERD, and ETH generation was still minor
408 compared to PZ-2. Curiously, the most inefficient ERD (*cis*-DCE stall confirmed by no

changes in its $\delta^{13}C_{cis\text{-DCE}}$ after t_{50}) of these wells occurred in PZ-1, where the initial drop in the Eh was followed by a rebound to more positive values after t_{86} (Figure S8D). In fact, as said before, according to sulphate isotopic composition, PZ-1 did not reach significant sulphate reducing conditions (Figure 3). This was most likely caused by the consumption and absence of electron donor from t_{86} onwards or fast entrance of oxidizing groundwater. In contrast, possibly due to the combination of preferential flow paths and the influence of external active remediation systems (P&T and DPE) on the groundwater flow direction, certain amounts of organic acids arrived to wells PZ-6 and MW-6 (Figure S9C, S10C), which were the farthest from PZ-2. Their Eh decreased much more progressively after t_{50}, and remained negative until t_{190}, allowing sulphate reducing conditions and further degradation to VC (Figure S9D, S10D).

3.2.4. Impact of the *in-situ* pilot test in wells outside the direct radius of influence

Lactate and acetate were not detected in wells PZ-3, PZ-22, and Prof.D (Figures S11C, S12C and S13C). Accordingly, Eh did not reach negative values in any of them (Figures S11D, S12D and S13D), not allowing to prove a direct effect of the ERD pilot test. In well PZ-3, Eh decreased to +60 mV at t_{86} but it rebounded to initial conditions at t_{190} (Figure S11D). Curiously, CEs concentrations decreased globally in PZ-3 and PZ-22, but PCE molar fraction increased in respect to its daughter products, which could indicate a solubilization and dilution of the PCE adsorbed to the soil due to the injected volume (Figure S14). Therefore, the ^{13}C enrichments observed for TCE and *cis*-DCE in PZ-3 (by +11.5‰ and +8.1‰, respectively, Figure S11) could be attributed to reductive dechlorination in the well or, most probably, associated to the dispersion from upstream contaminants (Figure 1). In wells PZ-22 and Prof.D, changes in CEs concentrations (Figures S12A and S13A) were not associated to significant shifts in ^{13}C values (Figures S12B and S13B), confirming this dilution effect.

435 3.2.5. Changes in the native microbial community induced by the *in-situ* pilot test

436 The effect of lactate injection on the microbial community of the aquifer was
437 investigated by high-throughput sequencing of the 16S rRNA region of selected
438 groundwater samples. PZ-2, PZ-1 and PZ-22 at t_{-1} and t_{142} were chosen based on the
439 results obtained in the pilot test, as they represented three different scenarios: i) PCE-to-
440 ETH reaction at the injection well (PZ-2), ii) *cis*-DCE stall (PZ-1), and iii) a well not
441 directly impacted by the injection of lactate (PZ-22). In PZ-2, the most abundant phyla at
442 t_{-1} were *Proteobacteria* (58%), *Planctomycetes* (11%), *Bacteroidetes* (6%),
443 *Verrucomicrobia* (6%), *Chlamydiae* (4%), *Actinobacteria* (4%), and *Acidobacteria* (2%),
444 whereas at t_{142}, the community shifted to *Firmicutes* (67%), *Bacteroidetes* (14%),
445 *Proteobacteria* (14%), and *Tenericutes* (2%) (Figure 6, Table S4). Within *Firmicutes*,
446 bacteria from the family *Veillonellaceae* (26%), and *Erysipelotrichaceae* (9%) were the
447 most abundant; and the same occurred for the genus *Desulfovibrio* (3%), from the
448 *Proteobacteria* phylum (data not shown). The microbial composition after the injection
449 of lactate was dominated by fermenting bacteria that were probably induced by the
450 injection of lactate (Fennell et al., 1997; He et al., 2007; Tegtmeier et al., 2016). In
451 contrast, the abundance of the *Firmicutes* phylum was very limited in well PZ-1
452 (abundance of 4% at t_{142}) and almost insignificant in well PZ-22, which agrees with the
453 chemical and isotopic results discussed before.

454 *3.3. Isotopic evaluation of the full-scale ERD with lactate*

455 After the *in-situ* ERD pilot test, which finished in June 2017, a full-scale ERD with
456 Lactate-2 was implemented on August 2017. After one year of full-scale treatment (from
457 August 2017 to September 2018), an isotopic mass balance of CEs was calculated from
458 6 selected monitoring wells (PZ-3, PZ-5, PZ-22, MW-3, MW-6, MW-7, Figure 1) to
459 evaluate the extent and success of the full-scale ERD. Results revealed that PCE and TCE
460 were completely depleted in 5 out of the 6 monitoring wells and VC and ETH were the

major end products (Table 1). Originally, $\delta^{13}C_{sum}$ at the site was, in average, of -30 ± 2‰, which responded to the original $\delta^{13}C$ value of PCE (Blázquez-Pallí et al., 2019). After one year of full-scale ERD, the $\delta^{13}C_{sum}$ values in those 5 wells were enriched (ranging from -23.2 ± 0.5‰ to -13 ± 1‰) with respect to the initial value (Table 1). This trend in $\delta^{13}C_{sum}$ of becoming more positive was also observed in well PZ-2 during the *in-situ* pilot test and responds to ETH production. In the case of MW-7, the $\delta^{13}C_{sum}$ was already different from the rest of the wells in the characterization campaign (May 2016) (Blázquez-Pallí et al., 2019), but biodegradation up to VC has been also observed after the full-scale (Table 1). Therefore, these results confirmed that the reductive dechlorination of CEs was occurring across the site, albeit at different extent in each well.

4. Conclusions

The present study aimed at validating a multidisciplinary methodology to assess and monitor biodegradation of CEs at the field scale. In this work, hydrochemical, isotopic and microbiological data from the field was examined together with aquifer-derived laboratory microcosms to get an insight into the idiosyncrasies of the aquifer. The first part of this study focused on the diagnosis of the *in-situ* biodegradation potential of the site for full reductive dechlorination of CEs. The results obtained provided evidence that the stall at *cis*-DCE and VC was due to the lack of electron donors. Afterwards, the injection of lactate in a monitoring well evidenced that full reductive dechlorination to ETH was achieved within 190 days, and that the reaction followed a different pace in the surrounding monitoring wells. Therefore, the hydrodynamic characteristics of the aquifer possibly dominated the distribution of electron donor, hence, affecting the outcome of the biodegradation reaction in the studied surrounding wells. The methodology proposed here can be easily integrated as a tool in the early stages of site investigation to decide which bioremediation strategy is more suitable according to the specific characteristics of the

aquifer. Moreover, it can reduce the uncertainties regarding the ongoing processes that are occurring in groundwater systems. Finally, the initial isotopic characterization of the site allowed for applying isotope-mass balance calculations to unequivocally demonstrate ETH generation after the full-scale enhanced reductive dechlorination via lactate injection. This stable isotope-based technique can overcome the difficulties related to the traditional mass balance approaches which are often hindered by natural processes (e.g. dilution, sorption, volatilization).

5. Acknowledgements

This research has been supported by *Agencia Estatal de Investigación* (CTM2016-75587-C2-1-R, CGL2014-57215-C4-1-R and CGL2017-87216-C4-1-R projects) and co-financed by the European Union through the European Regional Development Fund (ERDF). This work was also partly supported by *Generalitat de Catalunya* through the consolidate research groups (2017-SGR-14 and 2017SGR-1733) and the Industrial Doctorate grant (2015-DI-064) of N. Blázquez-Pallí. M. Rosell acknowledges a *Ramón y Cajal* contract (RYC-2012-11920) from MINECO. The *Departament d'Enginyeria Química, Biològica i Ambiental* of *Universitat Autònoma de Barcelona* is a member of *Xarxa de Referència en Biotecnologia de la Generalitat de Catalunya*. We thank Dr. Ivonne Nijenhuis for providing *Dehalococcoides mccartyi* BTF08, Dr. Cristina Domènech for the geochemical modelling advice, David Fernández-Verdejo for his contribution in the laboratory work, and CCiT-UB and Dr. Roger Puig for excellent technical assistance.

Figure 1. Water table (blue lines, in m.a.s.l.) representative of the natural groundwater flow at the site and location of monitoring wells. Red numerical codes refer to the wells monitored during the *in-situ* ERD pilot test.

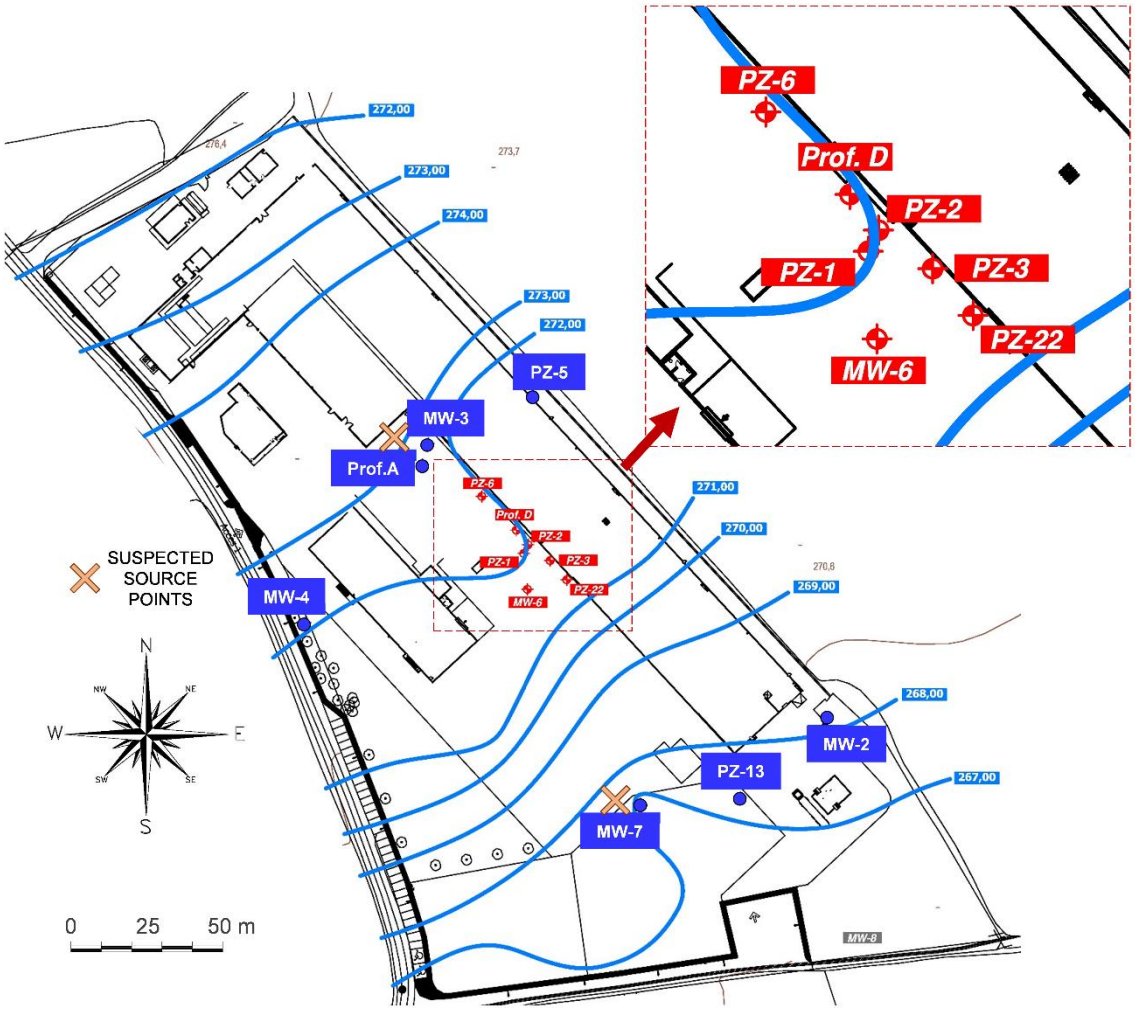

Figure 2. Microbial population in enriched cultures derived from microcosms amended with Lactate-2 from well PZ-2. Average composition obtained from two cultures (A and B) that were enriched with TCE first, and later with *cis*-DCE for several consecutive dilution series. Total sequence reads for the genera *Geobacter* and *Dehalococcoides* were, respectively, 24232/140088 and 5393/140088 in replicate A, and 10421/103805 and 3023/103805 in replicate B. Genera with abundance <1% are grouped in "Other".

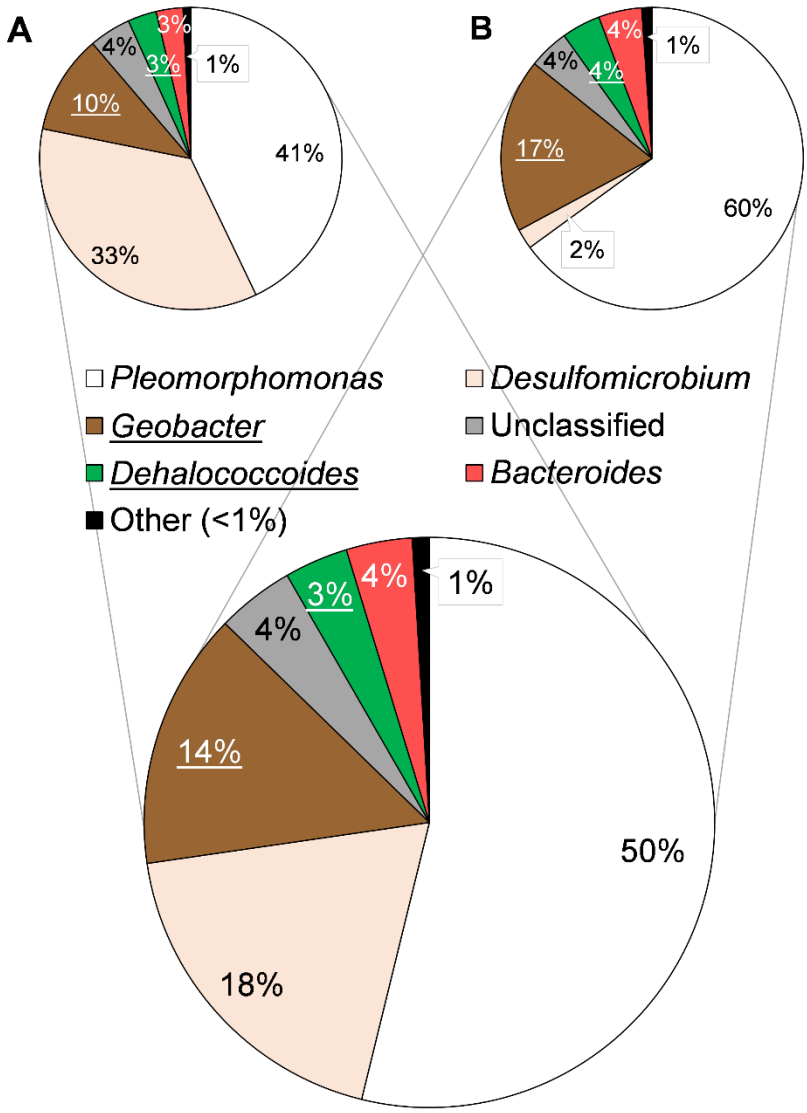

Figure 3. Dual S–O isotopic compositions of SO_4^{-2} during the *in-situ* ERD pilot test in all monitored wells. "Injected water" refers to the groundwater collected from across the aquifer, treated through an air stripping system, later mixed with Lactate-2, and injected into well PZ-2 for the pilot test. Samples t_{86} and t_{190} for PZ-2 had too low SO_4^{-2} concentration for isotopic measurements, while sample t_{86} for PZ-6 was lost. Dashed black lines represent the slopes estimated for each well with the available values. Shapes of symbols indicate different sampling events, while colours indicate different monitoring wells.

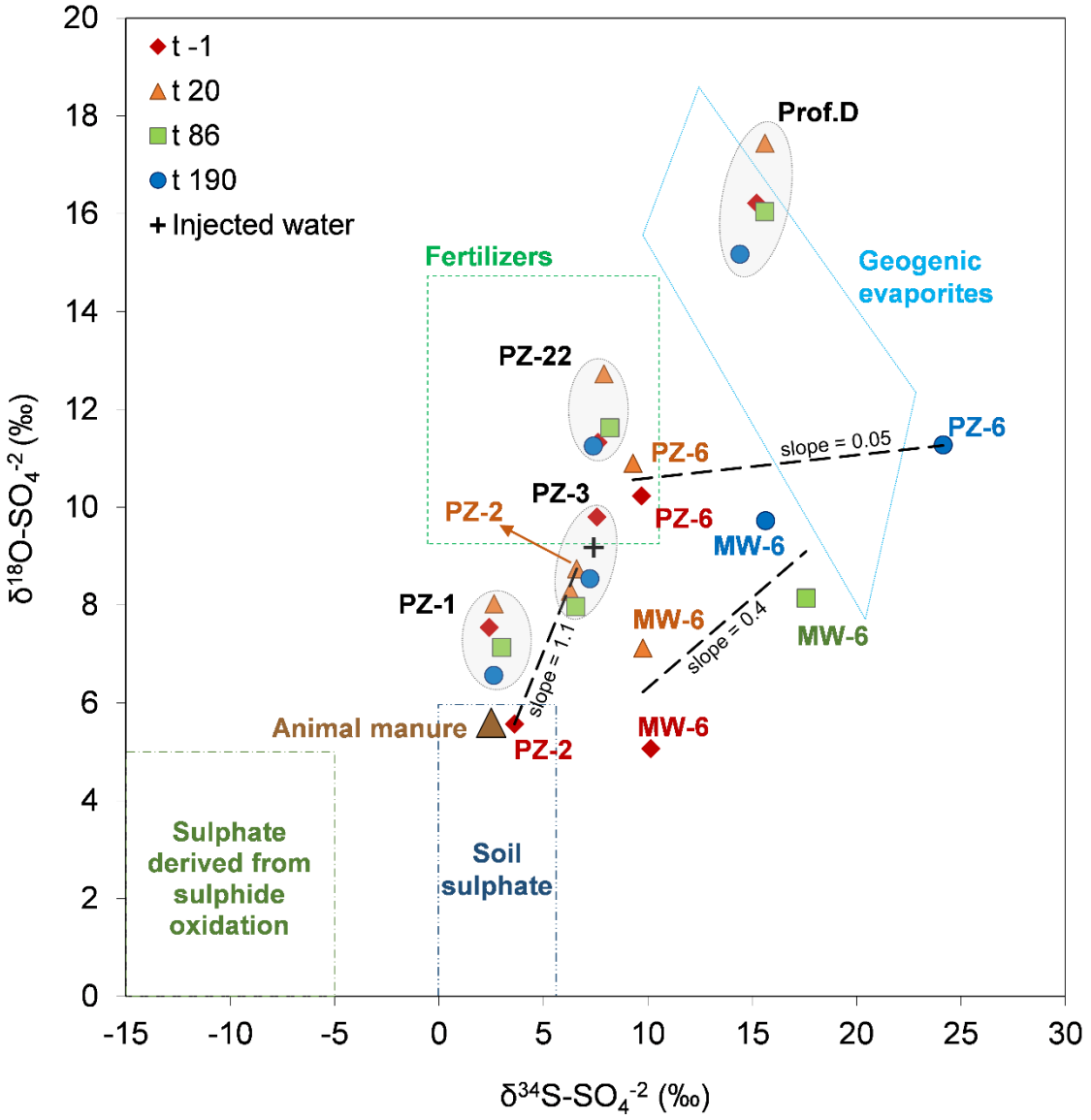

Figure 4. Time-course of monitored parameters at well PZ-2 during the *in-situ* pilot test: (A) concentration of CEs; (B) carbon isotopic composition and balance; (C) concentration of organic acids, and (D) redox potential (Eh). Data presented is an average of each sampling event and includes error bars showing the one standard deviation (1σ) for duplicate measurements.

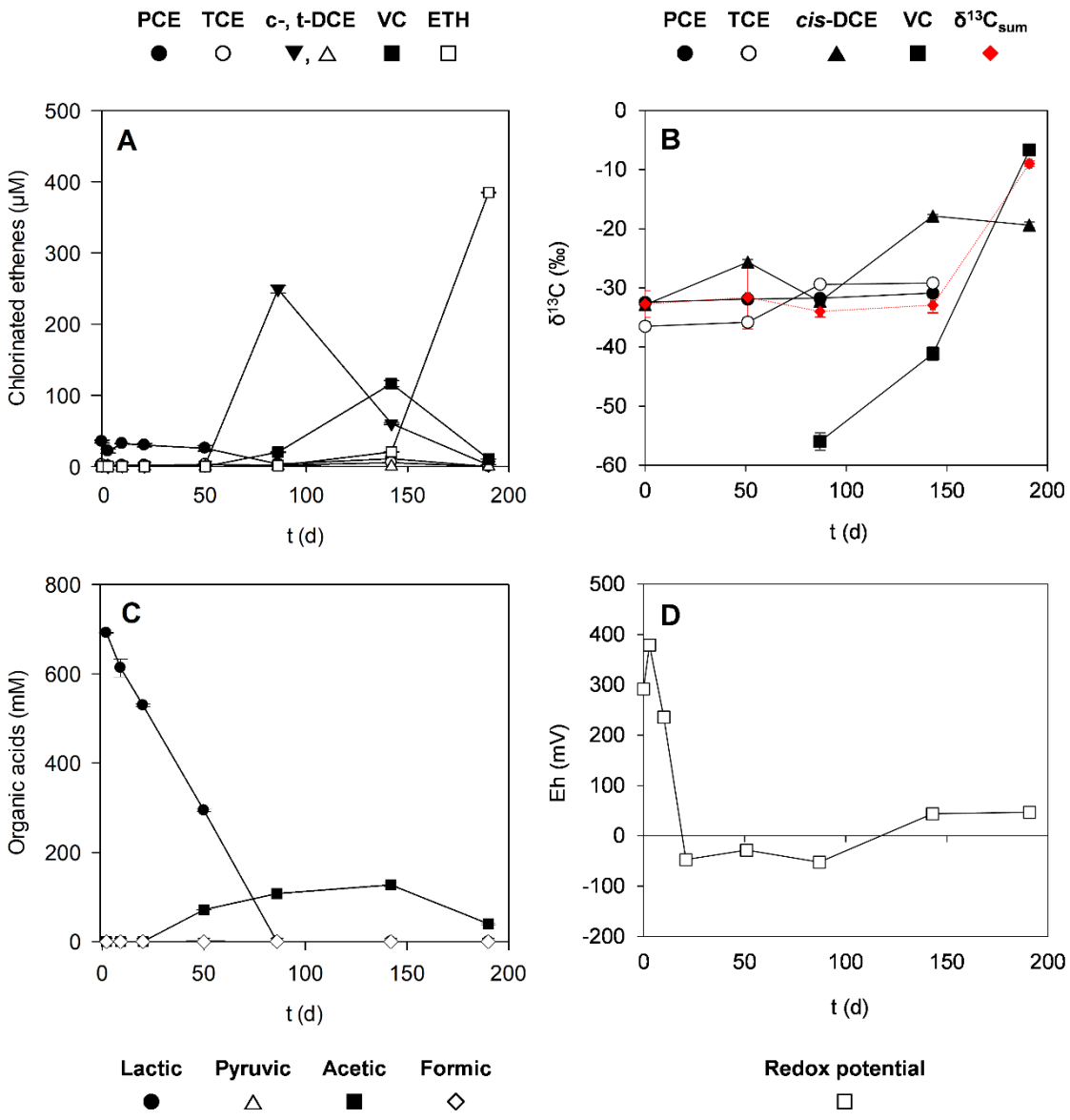

Figure 5. Location of the lactate injection well (PZ-2) and the monitoring wells of the *in-situ* ERD pilot test where the influence of the biostimulation was proved along 190 days, indicating the molar fraction shift of CEs + ETH and the final carbon isotopic mass balance ($\delta^{13}C_{sum,t190}$). The size of the pie charts is related to the total concentration of CEs + ETH in each well and sampling time. For more detailed results, see Figures 4, S8, S9 and S10.

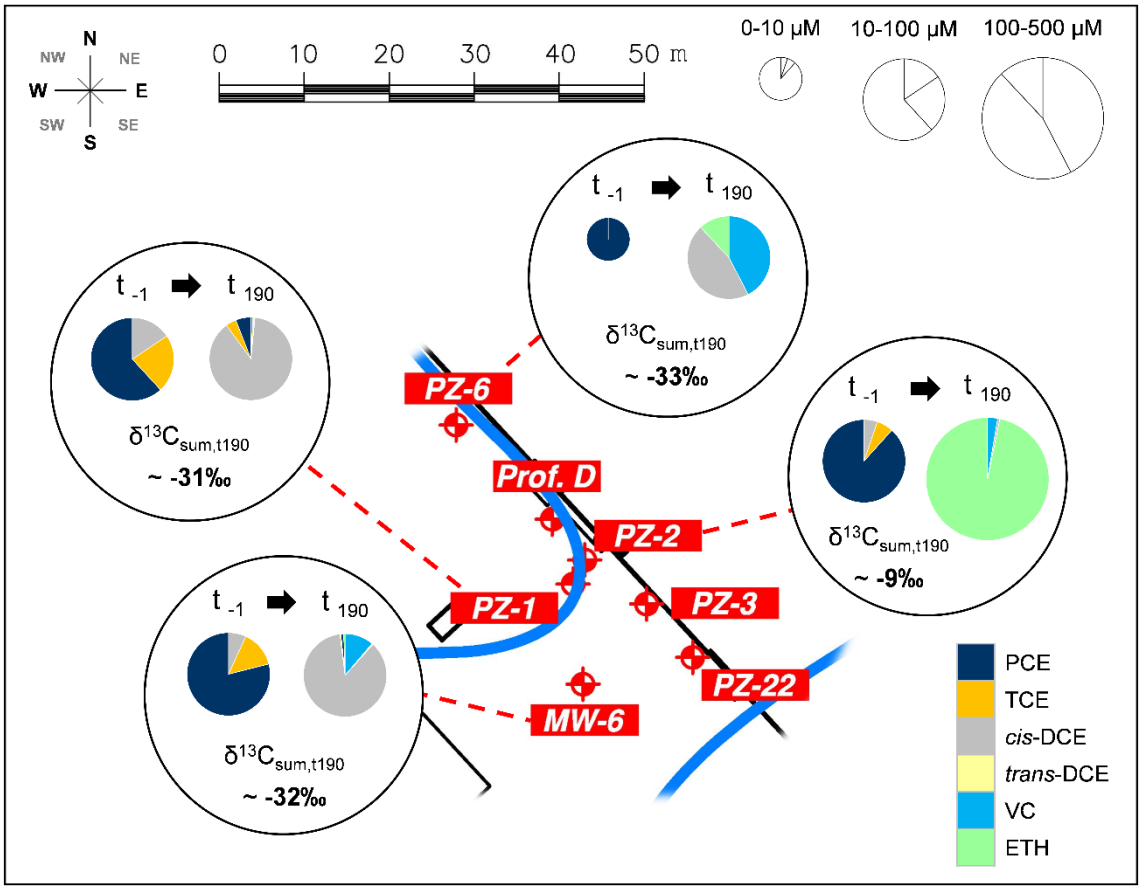

Figure 6. 16S rRNA high-throughput sequencing results at the phylum level for wells PZ-2, PZ-1, and PZ-22 before lactate injection (t_{-1}) and after injection (t_{142}). Detailed abundance (in %) is presented in Table S4. Phyla in bold are the most abundant in PZ-2 (either at t_{-1} or t_{142}).

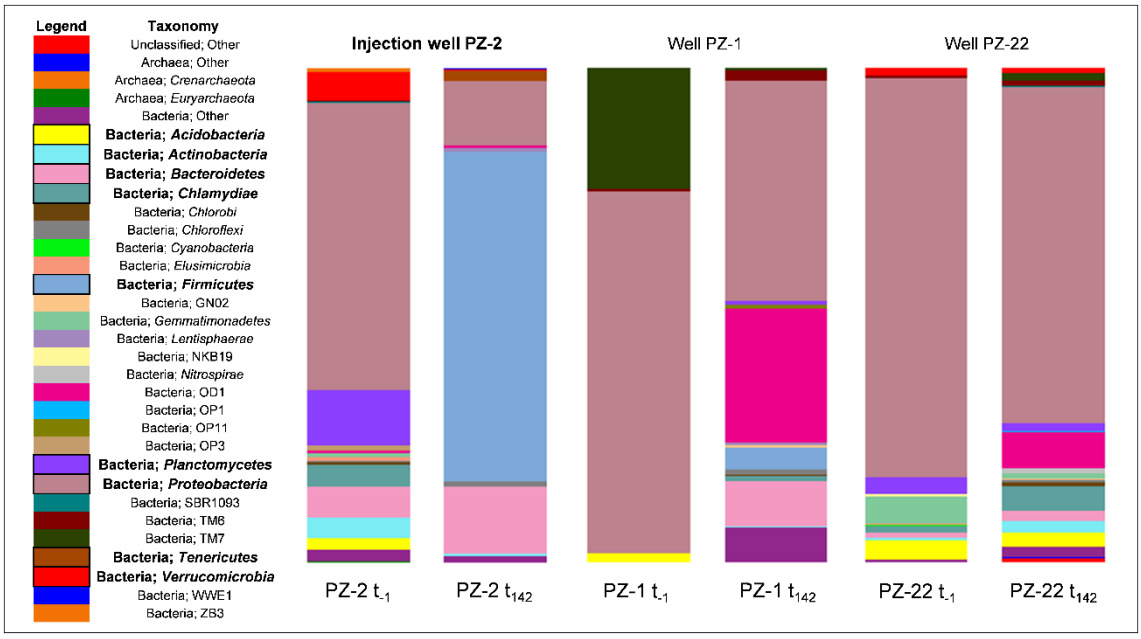

583 **References**

584 Adrian, L., Löffler, F.E., 2016. Organohalide-Respiring Bacteria, Organohalide-
585 Respiring Bacteria. Springer Berlin Heidelberg, Berlin, Heidelberg.
586 https://doi.org/10.1007/978-3-662-49875-0

587 Aelion, C.M., Höhener, P., Hunkeler, D., Aravena, R., 2009. Environmental Isotopes in
588 Bioremediation and Biodegradation. CRC Press, Boca Raton.
589 https://doi.org/10.1159/000076616

590 Aeppli, C., Hofstetter, T.B., Amaral, H.I.F., Kipfer, R., Schwarzenbach, R.P., Berg, M.,
591 2010. Quantifying in situ transformation rates of chlorinated ethenes by combining
592 compound-specific stable isotope analysis, groundwater dating, and carbon isotope
593 mass balances. Environ. Sci. Technol. 44, 3705–3711.
594 https://doi.org/10.1021/es903895b

595 Antler, G., Turchyn, A. V, Rennie, V., Herut, B., Sivan, O., 2013. Coupled sulfur and
596 oxygen isotope insight into bacterial sulfate reduction in the natural environment.
597 Geochim. Cosmochim. Acta 118, 98–117.
598 https://doi.org/10.1016/j.gca.2013.05.005

599 Atashgahi, S., Lu, Y., Smidt, H., 2016. Overview of known organohalide-respiring
600 bacteria-phylogenetic diversity and environmental distribution, in: L. Adrian and
601 F.E. Löffler (Ed) Organohalide-Respiring Bacteria. Springer Berlin Heidelberg,
602 Berlin, Heidelberg, pp. 63–105. https://doi.org/10.1007/978-3-662-49875-0_5

603 ATSDR, 2017. Substance Priority List [WWW Document]. Agency Toxic Subst. Dis.
604 Regist. URL https://www.atsdr.cdc.gov/SPL/index.html#2017spl (accessed
605 4.17.19).

606 Blázquez-Pallí, N., Rosell, M., Varias, J., Bosch, M., Soler, A., Vicent, T., Marco-

607 Urrea, E., 2019. Multi-method assessment of the intrinsic biodegradation potential
608 of an aquifer contaminated with chlorinated ethenes at an industrial area in
609 Barcelona (Spain). Environ. Pollut. 244, 165–173.
610 https://doi.org/10.1016/j.envpol.2018.10.013

611 Bradley, P.M., 2000. Microbial degradation of chloroethenes in groundwater systems.
612 Hydrogeol. J. 8, 251–253. https://doi.org/10.1007/s100400050011

613 Buchner, D., Behrens, S., Laskov, C., Haderlein, S.B., 2015. Resiliency of stable
614 isotope fractionation (δ13C and δ37Cl) of trichloroethene to bacterial growth
615 physiology and expression of key enzymes. Environ. Sci. Technol. 49, 13230–
616 13237. https://doi.org/10.1021/acs.est.5b02918

617 Cichocka, D., Imfeld, G., Richnow, H.H., Nijenhuis, I., 2008. Variability in microbial
618 carbon isotope fractionation of tetra- and trichloroethene upon reductive
619 dechlorination. Chemosphere 71, 639–648.
620 https://doi.org/10.1016/j.chemosphere.2007.11.013

621 Courbet, C., Rivière, A., Jeannottat, S., Rinaldi, S., Hunkeler, D., Bendjoudi, H., de
622 Marsily, G., 2011. Complementing approaches to demonstrate chlorinated solvent
623 biodegradation in a complex pollution plume: Mass balance, PCR and compound-
624 specific stable isotope analysis. J. Contam. Hydrol. 126, 315–329.
625 https://doi.org/10.1016/j.jconhyd.2011.08.009

626 Dogramaci, S.., Herczeg, A.., Schiff, S.., Bone, Y., 2001. Controls on δ 34 S and δ 18 O
627 of dissolved sulfate in aquifers of the Murray Basin, Australia and their use as
628 indicators of flow processes. Appl. Geochemistry 16, 475–488.
629 https://doi.org/10.1016/S0883-2927(00)00052-4

630 Dugat-Bony, E., Biderre-Petit, C., Jaziri, F., David, M.M., Denonfoux, J., Lyon, D.Y.,
631 Richard, J.-Y., Curvers, C., Boucher, D., Vogel, T.M., Peyretaillade, E., Peyret, P.,

2012. In situ TCE degradation mediated by complex dehalorespiring communities during biostimulation processes. Microb. Biotechnol. 5, 642–653. https://doi.org/10.1111/j.1751-7915.2012.00339.x

Ebert, K., Laskov, C., Behrens, S., Haderlein, S.B., 2010. Assessment of chlorinated ethenes biodegradation in an anaerobic aquifer by isotope analysis and microcosm studies. IAHS Publ 342, 13–18.

Elsner, M., 2010. Stable isotope fractionation to investigate natural transformation mechanisms of organic contaminants: principles, prospects and limitations. J. Environ. Monit. 12, 2005–2031. https://doi.org/10.1039/c0em00277a

European Commission, 2008. Directive 2008/105/EC of 16 December 2008 on environmental quality standards in the field of water policy, Official Journal of the European Union. https://doi.org/http://eur-lex.europa.eu/legal-content/EN/TXT/?uri=celex:32008L0105

Fennell, D.E., Gossett, J.M., Zinder, S.H., 1997. Comparison of butyric acid, ethanol, lactic acid, and propionic acid as hydrogen donors for the reductive dechlorination of tetrachloroethene. Environ. Sci. Technol. 31, 918–926. https://doi.org/10.1021/es960756r

He, J., Holmes, V.F., Lee, P.K.H., Alvarez-Cohen, L., 2007. Influence of vitamin B12 and cocultures on the growth of Dehalococcoides isolates in defined medium. Appl. Environ. Microbiol. 73, 2847–2853. https://doi.org/10.1128/AEM.02574-06

Herlemann, D.P.R., Labrenz, M., Jürgens, K., Bertilsson, S., Waniek, J.J., Andersson, A.F., 2011. Transitions in bacterial communities along the 2000 km salinity gradient of the Baltic Sea. ISME J. 5, 1571–1579. https://doi.org/10.1038/ismej.2011.41

656 Hermon, L., Denonfoux, J., Hellal, J., Joulian, C., Ferreira, S., Vuilleumier, S., Imfeld,
657 G., 2018. Dichloromethane biodegradation in multi-contaminated groundwater:
658 Insights from biomolecular and compound-specific isotope analyses. Water Res.
659 142, 217–226. https://doi.org/10.1016/j.watres.2018.05.057

660 Hermon, L., Hellal, J., Denonfoux, J., Vuilleumier, S., Imfeld, G., Urien, C., Ferreira,
661 S., Joulian, C., 2019. Functional genes and bacterial communities during
662 organohalide respiration of chloroethenes in microcosms of multi-contaminated
663 groundwater. Front. Microbiol. 10, 89. https://doi.org/10.3389/fmicb.2019.00089

664 Herrero, J., Puigserver, D., Nijenhuis, I., Kuntze, K., Carmona, J.M., 2019. Combined
665 use of ISCR and biostimulation techniques in incomplete processes of reductive
666 dehalogenation of chlorinated solvents. Sci. Total Environ. 648, 819–829.
667 https://doi.org/10.1016/j.scitotenv.2018.08.184

668 Hirschorn, S.K., Grostern, A., Lacrampe-Couloume, G., Edwards, E.A., MacKinnon,
669 L., Repta, C., Major, D.W., Sherwood Lollar, B., 2007. Quantification of
670 biotransformation of chlorinated hydrocarbons in a biostimulation study: Added
671 value via stable carbon isotope analysis. J. Contam. Hydrol. 94, 249–260.
672 https://doi.org/10.1016/j.jconhyd.2007.07.001

673 Hunkeler, D., Aravena, R., Butler, B.J., 1999. Monitoring microbial dechlorination of
674 tetrachloroethene (PCE) in groundwater using compound-specific stable carbon
675 isotope ratios: Microcosm and field studies. Environ. Sci. Technol. 33, 2733–2738.
676 https://doi.org/10.1021/es981282u

677 Hunkeler, D., Meckenstock, R.U., Lollar, B.S., Schmidt, T.C., Wilson, J.T., 2008. A
678 guide for assessing biodegradation and source identification of organic ground
679 water contaminants using compound specific isotope analysis (CSIA), U.S.
680 Environmental Protection Agency. Washington, D.C., EPA/600/R-08/148.

681 Im, W.T., Kim, S.H., Kim, M.K., Ten, L.N., Lee, S.T., 2006. Pleomorphomonas
682 koreensis sp. nov., a nitrogen-fixing species in the order Rhizobiales. Int. J. Syst.
683 Evol. Microbiol. 56, 1663–1666. https://doi.org/10.1099/ijs.0.63499-0

684 Klindworth, A., Pruesse, E., Schweer, T., Peplies, J., Quast, C., Horn, M., Glöckner,
685 F.O., 2013. Evaluation of general 16S ribosomal RNA gene PCR primers for
686 classical and next-generation sequencing-based diversity studies. Nucleic Acids
687 Res. 41, e1–e1. https://doi.org/10.1093/nar/gks808

688 Kuder, T., Van Breukelen, B.M., Vanderford, M., Philp, P., 2013. 3D-CSIA: Carbon,
689 chlorine, and hydrogen isotope fractionation in transformation of TCE to ethene by
690 a dehalococcoides culture. Environ. Sci. Technol. 47, 9668–9677.
691 https://doi.org/10.1021/es400463p

692 Lee, J., Im, J., Kim, U., Löffler, F.E., 2016. A data mining approach to predict in situ
693 detoxification potential of chlorinated ethenes. Environ. Sci. Technol. 50, 5181–
694 5188. https://doi.org/10.1021/acs.est.5b05090

695 Leeson, A., Beevar, E., Henry, B.M., Fortenberry, J., Coyle, C., Parsons Corp., 2004.
696 Principles and practices of enhanced anaerobic bioremediation of chlorinated
697 solvents. Port Hueneme, California, ESTCP CU 0125.

698 Leys, D., Adrian, L., Smidt, H., 2013. Organohalide respiration: microbes breathing
699 chlorinated molecules. Philos. Trans. R. Soc. Lond. B. Biol. Sci. 368, 20120316.
700 https://doi.org/10.1098/rstb.2012.0316

701 Löffler, F.E., Sanford, R.A., Ritalahti, K.M., 2005. Enrichment, cultivation, and
702 detection of reductively dechlorinating bacteria. Methods Enzymol. 397, 77–111.
703 https://doi.org/10.1016/S0076-6879(05)97005-5

704 Lu, X., Wilson, J.T., Kampbell, D.H., 2009. Comparison of an assay for

705 Dehalococcoides DNA and a microcosm study in predicting reductive
706 dechlorination of chlorinated ethenes in the field. Environ. Pollut. 157, 809–815.
707 https://doi.org/10.1016/j.envpol.2008.11.015

708 Madhaiyan, M., Jin, T.Y., Roy, J.J., Kim, S.-J., Weon, H.-Y., Kwon, S.-W., Ji, L., 2013.
709 Pleomorphomonas diazotrophica sp. nov., an endophytic N-fixing bacterium
710 isolated from root tissue of Jatropha curcas L. Int. J. Syst. Evol. Microbiol. 63,
711 2477–2483. https://doi.org/10.1099/ijs.0.044461-0

712 Martín-González, L., Mortan, S.H., Rosell, M., Parladé, E., Martínez-Alonso, M., Gaju,
713 N., Caminal, G., Adrian, L., Marco-Urrea, E., 2015. Stable carbon isotope
714 fractionation during 1,2-dichloropropane-to-propene transformation by an
715 enrichment culture containing Dehalogenimonas strains and a dcpA gene. Environ.
716 Sci. Technol. 49, 8666–74. https://doi.org/10.1021/acs.est.5b00929

717 Matteucci, F., Ercole, C., Del Gallo, M., 2015. A study of chlorinated solvent
718 contamination of the aquifers of an industrial area in central Italy: A possibility of
719 bioremediation. Front. Microbiol. 6, 1–10.
720 https://doi.org/10.3389/fmicb.2015.00924

721 Mizutani, Y., Rafter, T.A., 1973. Isotopic behaviour of sulphate oxygen in the bacterial
722 reduction of sulphate. Geochem. J. 6, 183–191.
723 https://doi.org/10.2343/geochemj.6.183

724 Mortan, S.H., Martín-González, L., Vicent, T., Caminal, G., Nijenhuis, I., Adrian, L.,
725 Marco-Urrea, E., 2017. Detoxification of 1,1,2-trichloroethane to ethene in a
726 bioreactor co-culture of Dehalogenimonas and Dehalococcoides mccartyi strains. J.
727 Hazard. Mater. 331, 218–225. https://doi.org/10.1016/j.jhazmat.2017.02.043

728 Nijenhuis, I., Nikolausz, M., Köth, A., Felföldi, T., Weiss, H., Drangmeister, J.,
729 Großmann, J., Kästner, M., Richnow, H.H., 2007. Assessment of the natural

730 attenuation of chlorinated ethenes in an anaerobic contaminated aquifer in the
731 Bitterfeld/Wolfen area using stable isotope techniques, microcosm studies and
732 molecular biomarkers. Chemosphere 67, 300–311.
733 https://doi.org/10.1016/j.chemosphere.2006.09.084

734 Otero, N., Soler, A., Canals, À., 2008. Controls of δ34S and δ18O in dissolved sulphate:
735 learning from a detailed survey in the Llobregat River (Spain). Appl. Geochemistry
736 23, 1166–1185. https://doi.org/10.1016/j.apgeochem.2007.11.009

737 Palau, J., Marchesi, M., Chambon, J.C.C., Aravena, R., Canals, À., Binning, P.J., Bjerg,
738 P.L., Otero, N., Soler, A., 2014. Multi-isotope (carbon and chlorine) analysis for
739 fingerprinting and site characterization at a fractured bedrock aquifer contaminated
740 by chlorinated ethenes. Sci. Total Environ. 475, 61–70.
741 https://doi.org/10.1016/j.scitotenv.2013.12.059

742 Puigdomènech, I., 2010. MEDUSA (Make Equilibrium Diagrams Using Sophisticated
743 Algorithms) Windows interface to the MS-DOS versions of INPUT, SED and
744 PREDOM (FORTRAN programs drawing chemical equilibrium diagrams) Vers. 6
745 Dec 2010. R. Inst. Technol. Stock. Sweden.

746 Rodríguez-Fernández, D., Torrentó, C., Palau, J., Marchesi, M., Soler, A., Hunkeler, D.,
747 Domènech, C., Rosell, M., 2018. Unravelling long-term source removal effects and
748 chlorinated methanes natural attenuation processes by C and Cl stable isotopic
749 patterns at a complex field site. Sci. Total Environ. 645, 286–296.
750 https://doi.org/10.1016/j.scitotenv.2018.07.130

751 Sanford, R.A., Chowdhary, J., Löffler, F.E., 2016. Organohalide-respiring
752 Deltaproteobacteria, in: L. Adrian and F.E. Löffler (Ed) Organohalide-Respiring
753 Bacteria. Springer Berlin Heidelberg, Berlin, Heidelberg, pp. 235–258.
754 https://doi.org/10.1007/978-3-662-49875-0_11

Scheutz, C., Durant, N.D., Dennis, P., Hansen, M.H., Jørgensen, T., Jakobsen, R., Cox, E. e., Bjerg, P.L., 2008. Concurrent ethene generation and growth of Dehalococcoides containing vinyl chloride reductive dehalogenase genes during an enhanced reductive dechlorination field demonstration. Environ. Sci. Technol. 42, 9302–9309. https://doi.org/10.1021/es800764t

Sharak Genthner, B.R., Friedman, S.D., Devereux, R., 1997. Reclassification of Desulfovibrio desulfuricans Norway 4 as Desulfomicrobium norvegicum comb. nov. and confirmation of Desulfomicrobium escambiense (corrig. Int. J. Syst. Bacteriol. 47, 889–892.

Sharak Genthner, B.R., Mundfrom, G., Devereux, R., 1994. Characterization of Desulfomicrobium escambium sp. nov. and proposal to assign Desulfovibrio desulfuricans strain Norway 4 to the genus Desulfomicrobium. Arch. Microbiol. 161, 215–219. https://doi.org/10.1007/BF00248695

Sherwood Lollar, Barbara, Hirschorn, S.K., Chartrand, M.M.G., Lacrampe-Couloume, G., Sherwood Lollar, B., 2007. An approach for assessing total instrumental uncertainty in compound-specific carbon isotope analysis: implications for environmental remediation studies. Anal. Chem. 79, 3469–3475. https://doi.org/10.1021/ac062299v

Slater, G.F., Sherwood Lollar, Barbara, Sleep, B.E., Edwards, E.A., Sherwood Lollar, B., 2001. Variability in carbon isotopic fractionation during biodegradation of chlorinated ethenes: implications for field applications. Environ. Sci. Technol. 35, 901–907. https://doi.org/10.1021/es001583f

Song, D.L., Conrad, M.E., Sorenson, K.S., Alvarez-Cohen, L., 2002. Stable carbon isotope fractionation during enhanced in situ bioremediation of trichloroethene. Environ. Sci. Technol. 36, 2262–2268. https://doi.org/10.1021/es011162d

780 Stroo, H.F., Ward, C.H., 2010. In situ remediation of chlorinated solvent plumes, 1st ed,
781 SERDP/ESTCP Environmental Remediation Technology. Springer New York,
782 New York, NY. https://doi.org/10.1007/978-1-4419-1401-9

783 Tarnawski, S.-E., Rossi, P., Brennerova, M. V., Stavelova, M., Holliger, C., 2016.
784 Validation of an Integrative Methodology to Assess and Monitor Reductive
785 Dechlorination of Chlorinated Ethenes in Contaminated Aquifers. Front. Environ.
786 Sci. 4, 1–16. https://doi.org/10.3389/fenvs.2016.00007

787 Tegtmeier, D., Riese, C., Geissinger, O., Radek, R., Brune, A., 2016. Breznakia
788 blatticola gen. nov. sp. nov. and Breznakia pachnodae sp. nov., two fermenting
789 bacteria isolated from insect guts, and emended description of the family
790 Erysipelotrichaceae. Syst. Appl. Microbiol. 39, 319–329.
791 https://doi.org/10.1016/j.syapm.2016.05.003

792 Wu, S., Jeschke, C., Dong, R., Paschke, H., Kuschk, P., Knöller, K., 2011. Sulfur
793 transformations in pilot-scale constructed wetland treating high sulfate-containing
794 contaminated groundwater: a stable isotope assessment. Water Res. 45, 6688–
795 6698. https://doi.org/10.1016/j.watres.2011.10.008

796 Xie, C.H., Yokota, A., 2005. Pleomorphomonas oryzae gen. nov., sp. nov., a nitrogen-
797 fixing bacterium isolated from paddy soil of Oryza sativa. Int. J. Syst. Evol.
798 Microbiol. 55, 1233–1237. https://doi.org/10.1099/ijs.0.63406-0

799 Yang, Y., Cápiro, N.L., Marcet, T.F., Yan, J., Pennell, K.D., Löffler, F.E., 2017a.
800 Organohalide respiration with chlorinated ethenes under low pH conditions.
801 Environ. Sci. Technol. 51, 8579–8588. https://doi.org/10.1021/acs.est.7b01510

802 Yang, Y., Higgins, S.A., Yan, J., Şimşir, B., Chourey, K., Iyer, R., Hettich, R.L.,
803 Baldwin, B.R., Ogles, D.M., Löffler, F.E., 2017b. Grape pomace compost harbors
804 organohalide-respiring Dehalogenimonas species with novel reductive

805 dehalogenase genes. ISME J. 11, 2767–2780.
806 https://doi.org/10.1038/ismej.2017.127

807 Yu, R., Andrachek, R.G., Lehmicke, L.G., Freedman, D.L., 2018. Remediation of
808 chlorinated ethenes in fractured sandstone by natural and enhanced biotic and
809 abiotic processes: A crushed rock microcosm study. Sci. Total Environ. 626, 497–
810 506. https://doi.org/10.1016/j.scitotenv.2018.01.064

811